Experimentally testing a generalized coarsening model for individual bubbles in quasi-two-dimensional wet foams

A. T. Chieco and D. J. Durian

Department of Physics and Astronomy, University of Pennsylvania, Philadelphia, Pennsylvania 19104-6396, USA

We present high-precision data for the time evolution of bubble area $A(t)$ and circularity shape parameter $C(t)$ for several bubbles in a quasi-two-dimensional foams consisting of bubbles squashed between parallel plates. In order to fully compare with earlier predictions, foam wetness is systematically varied by controlling the height of the sample above a liquid reservoir which in turn controls the radius r of the inflation of the Plateau borders. For very dry foams, where the borders are very small, classic von Neumann behavior is observed where a bubble's growth rate depends only on its number n of sides. For wet foams, the inflated borders impede gas exchange and cause deviations from von Neumann's law that are found to be in accord with the generalized coarsening equation. In particular, the overall growth rate varies linearly with the film height, which decrease as surface Plateau borders inflate. More interestingly, the deviation from $dA/dt \propto (n-6)$ von Neumann behavior grows in proportion to $nCr/\sqrt{A}$. This is highlighted definitively by data for six-sided bubbles, which are forbidden to grow or shrink except for the existence of this term. It is tested quantitatively by variation of all four relevant quantities: n, C, r, and A.

I. INTRODUCTION

Foams are out of equilibrium and made of bubbles that coarsen by the diffusion of gas across the soap films between neighboring bubbles of different pressure [1,2]. This occurs in both two-dimensional (2D) and three-dimensional (3D) systems and for any liquid content. Evolution kinetics like coarsening also occur in other cellular systems, but the macroscopic nature of bubbles and a known microstructure make foam an ideal system to study [3,4]. For ideally dry purely 2D foams, a bubble's area A changes at a rate that depends only on its number n of sides according to von Neumann's law [5]:

$$dA/dt = K_o(n-6), \tag{1}$$

where K_o is a rate constant dependent on the physical chemistry of the gas and the surfactant solution. This coarsening equation depends only on local topology and means that bubbles with less than six sides will shrink, bubbles with more than six sides will grow, and bubbles with exactly six sides will have constant area. The shrinking bubbles are small and eventually disappear leading to an overall increase in the average bubble area; there is an collective average growth rate, and eventually the foam enters a self-similar regime where size and topology distributions under proper normalization remain the same as the foam coarsens [6–14]. Whether the foam is or is not in a self similar state, the local coarsening rules for individual bubbles hold. However, the conditions for which Eq. (1) was developed cannot be met exactly by experiments on real foams which are necessarily wet and quasi-2D. An appropriate question is whether von Neumann's law can be modified in a way to account for these factors and accurately predict the behavior of individual bubbles as they coarsen in

wet foams. This is our focus, which underlies but is entirely separate from the question of self-similarity and the growth of the average bubble size.

We must first define the difference between "dry" and "wet" foams. In both cases the foams obey Plateau's laws, which are the structural criteria for foams in mechanical equilibrium. In two dimensions, Plateau's laws are as follows: films separating bubbles are circular arcs; films meet in threes at a vertex; the three films at a vertex are separated by equal angles of $120°$. In accordance with Plateau's laws bubbles are polygons with curved edges and vertices are all triconnected. A foam is "dry" if there is effectively zero liquid in films, Plateau borders, and vertices. Foam is "wet" if the both the Plateau borders and vertices are inflated with liquid [15]. Wet quasi-2D foams, where bubbles are squashed between parallel plates, also have liquid in surface Plateau borders along the top and bottom plates. These surface Plateau borders are connected by soap films of constant thickness, regardless of wetness [16–18]. Foams can also be "very wet" where there is a breakdown of Plateau's laws, and describing the foams in terms of inflated vertices and Plateau borders is no longer appropriate. Very wet foams have been studied in Ref. [19] with regard to their collective growth dynamics, and Ref. [20] develops a prediction for coarsening rates for individual bubbles but they are not considered here.

Any further discussion is therefore focused on dry and wet foams. Research on 2D and quasi-2D dry foams has been conducted in both experiment [7–9,21] and simulation [10–14,22], and general agreement with Eq. (1) is observed. However, there are instances where deviations from von Neumann's law are found; one such study explains such deviations by modifying von Neumann's law to account for

012610-1

differences from 120° of the internal angle at the vertices of a bubble [6]; this leads to an overall reduction in the coarsening rate. A later experiment reveals that removing much of the liquid from the foam makes it so the internal angles have no measurable differences from 120° and bubbles once again follow Eq. (1) for their coarsening dynamics [7]. These early experiments are evidence for the differences in coarsening behavior between wet and dry quasi-2D foam.

Theoretical work followed in Ref. [15] to show why wet foams coarsen more slowly; broadly they found that the liquid can entirely be decorated at the vertices of a 2D foam. However, the vertices grow in size with increasing liquid volume fraction; this reduces the length of the thin film faces between bubbles where gas diffuses and slows the overall coarsening rate. Additionally the liquid contained at the vertices can potentially change the turning angle, which provides a local quantity for deviations from von Neumann's law for individual bubbles.

These early experiments show that wetness indeed affects coarsening, but they were performed on foams where the coarsening rates are well approximated by von Neumann's law with only small deviations; the theoretical work relies on knowing the liquid volume fraction of the foam, which is notoriously difficult to measure in real systems and also focuses on purely 2D foams. Wet quasi-2D foams can have coarsening behavior much different than either of these cases because the surface Plateau borders run along the top and bottom plates of the cell and can swell with liquid. The swelling of the edges between bubbles was considered in simulation with a 2D Potts models [23] and in experiments on microfluidic foam [18]. These studies developed empirical formulas to describe the observed coarsening; still lacking were experiments that systematically test how liquid fraction affects foam coarsening and also develop some kind of modified von Neumann's law whose predictions about the coarsening of individual bubbles rely on the individual bubble-level topology and liquid content of the foam.

A pair of studies authored by previous members of this group sought to fill that void. Work from Ref. [16] modifies von Neumann's law for wet quasi-2D foams. This study finds an equation for coarsening that is derived by accounting for the size of the Plateau borders due to a higher liquid fraction foam and then going through the same topology based arguments as von Neumann. The resulting equation is developed for bubbles between two parallel plates separated by a distance H and makes two modifications to Eq. (1). The first is an overall reduced coarsening rate because gas does not diffuse through the Plateau borders enlarged by the liquid. The second is a modification to von Neumann's law due to the bubble shape and size. This model assumes gas does not diffuse at all through the Plateau border, i.e., "border blocking," but Ref. [20], the second work from the group, simulates gas flux through the surface Plateau borders. It finds the rate of gas diffusion is not zero and it is set by the geometric mean of the size of the Plateau border and the width of the thin film. Taking the shape and size dependent von Neumann modification from Ref. [16] and correcting its reduced coarsening rate for the amount of gas that diffuses through the surface Plateau borders found in Ref. [20] a prediction for how the area A of an n-sided bubble changes in time was developed.

This generalized coarsening equation is

$$\frac{dA}{dt} = K_o \left(1 - \frac{2r}{H} + \frac{\pi \sqrt{r\ell}}{H} \right) \left[(n-6) + \frac{6nCr}{\sqrt{3\pi A}} \right], \quad (2)$$

where $r = (r_t + r_b)/2$ is the average radius of curvature of the top and bottom surface Plateau borders, ℓ is the width of thin films that separate two bubbles, and C is a dimensionless shape parameter "circularity" of a bubble related to the curvature of the edges of bubble. For an n-sided bubble the circularity is

$$C = \left(\frac{1}{n} \sum_{i=1}^{n} \frac{1}{\mathcal{R}_i} \right) \sqrt{\frac{A}{\pi}}, \quad (3)$$

where $1/\mathcal{R}_i$ is the curvature of side i. Circularity is defined so it equals 1 for circular bubbles, is positive for convex bubbles, and is negative for concave bubbles. Experimentally, the average and standard deviation of the observed circularities were measured to be approximately $\langle C(n) \rangle = (1 - n/5.73) \pm 0.25$ in the self-similar scaling state [16]. Though there is significant variance in circularity between different bubbles of the same n, previous work compared only dA/dt data to expectation in terms of the average circularity.

Work from Ref. [16] shows that Eq. (2) accurately captures the coarsening behavior of bubbles in a wet foam on average; the data show there are deviations from von Neumann's law, and they are more pronounced for smaller wetter bubbles with $n < 6$. One other deviation that is apparent from Eq. (2) but only briefly mentioned in Ref. [16] is the fact that the generalized coarsening equation allows for the coarsening of six-sided bubbles. They do not show data for individual bubble coarsening in violation of von Neumann's law nor do they find how this coarsening is affected by the bubble specific shape and size. To explore the individual bubble dynamics in depth we develop alternative methods of image analysis to carefully reconstruct individual bubbles. From these reconstructions precise measurements of the bubble areas and circularities are obtained; the data are used to solve Eq. (2) and the solutions predict the unique shape-dependent coarsening of a bubble with great accuracy. We present data for individual six-sided bubbles that coarsen. This behavior is an obvious violation of Eq. (1), and it can be driven only by the bubble shape. Other bubbles with $n \neq 6$ either grow or shrink more slowly than predicted by von Neumann and in a nonlinear fashion; this behavior is also predicted by solutions to Eq. (2) and depends on the bubble size and circularity.

II. MATERIALS AND METHODS

Our experiments begin by making foam in a custom sample cell and allowing it to coarsen until it is quasi-2D. The custom sample cell, which has been used previously in Ref. [16], allows us to control the liquid content of the foams so we can systematically increase the wetness. As the foams increase in wetness the size of the surface Plateau borders inflates; however, all data are collected from foams that obey Plateaus laws, have vertices that are triconnected, and have bubbles that are polyhedra with faces separated by both thin films and surface Plateau borders. We take images of the foam over the course of many hours, and the images are used to reconstruct the

foam in a small neighborhood with high precision. The foams are reconstructed using in-house algorithms, and from the reconstructions the bubble areas and shapes are determined. We discuss these processes in the following subsections.

A. Experimental materials

The foaming solution is 92% deionized water and 8% Dawn Ultra Concentrated dish detergent and has a liquid-vapor surface tension $\gamma = 29 \pm 6$ dyn/cm. This solution generates stable foams that do not have any film ruptures. The foam is generated inside a sample cell constructed from two 1.91-cm-thick acrylic plates separated by a spacing $H = 0.32$ cm and sealed with two concentric o-rings; additional details about the specifications of the cell are found in Ref. [16] and in Fig. S1 of the Supplemental Material [24]. It features an annular trough that surrounds the foam and acts a reservoir for excess liquid drained from the foam due to gravity. The volume of the trough is large compared to the volume of liquid in the foam, so that the height d from the top of the liquid in the reservoir to the middle of the gap between the plates is constant. The value of d is then set by the amount of liquid sealed into the sample cell and serves as the key parameter controlling the wetness of the foam. Specifically, the foam drains into the reservoir, which causes the top and bottom surface Plateau border radii to decrease until capillary and gravitational pressures become equal:

$$\gamma/r_t = \rho g[(d + H/2) - r_t], \tag{4}$$

$$\gamma/r_b = \rho g[(d - H/2) + r_b]. \tag{5}$$

Here g is gravitational acceleration, and the terms in square brackets represent the distance from the liquid surface to the respective heights at which the surface Plateau borders begin to flare out from the soap film. These are the key heights which dominate the border-crossing gas flux [20]. For a chosen value of d, the surface Plateau border radii may thus be computed from these equations for use in Eq. (2).

Foams are produced as follows. First, the trough is filled with the desired amount of liquid, then flushed with nitrogen and sealed. The entire sample cell is vigorously shaken for several minutes until the gas is uniformly dispersed as fine bubbles that are small compared to the gap H between plates. The foam is thus initially very wet, opaque, and 3D. Immediately it begins to drain and coarsen, rapidly at first, then progressively more slowly as hydrostatic equilibrium is approached. After a few hours, the bubbles become large compared to the gap, and the coarsening rate is slow compared to drainage. Thereafter Eqs. (4) and (5) hold, and the foam is quasi-2D as desired for measurement. Figure 1 shows example images for three such foams with different d and hence different wetness. There it is evident that the border radii r significantly increase with decreasing d. Foams with these three wetnesses are used to garner all the data, and foams made using $d = \{11.4, 5.9, 3.5\}$ mm have approximate liquid volume fraction $\phi = \{0.01, 0.03, 0.06\}$; we note these volume fractions are imprecise but are important to show they are all relatively small and have the same order of magnitude. Furthermore, the real figure of merit for wetness in a quasi-
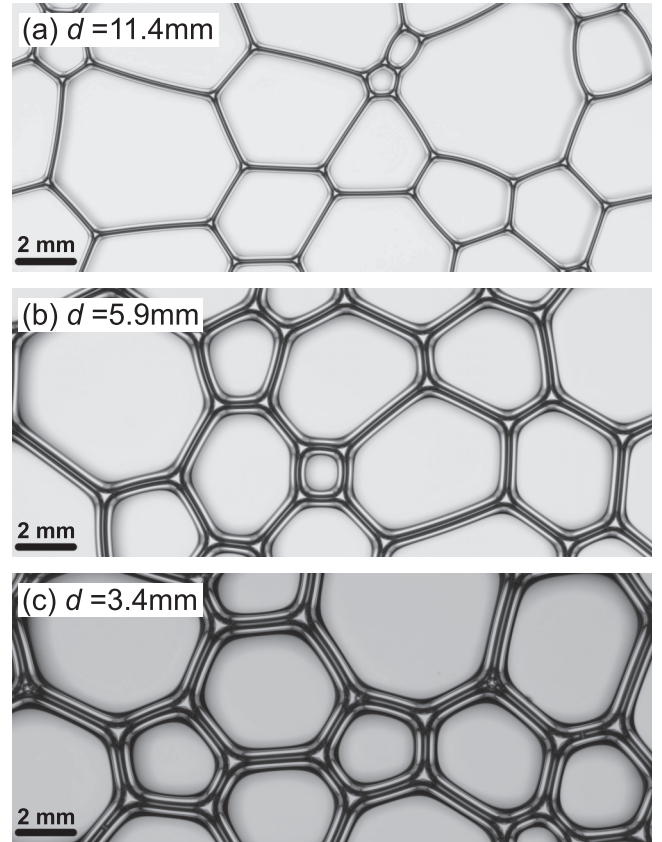

FIG. 1. Top down view of quasi-2D foams of various liquid content as indicated by the distance d from top surface of liquid in the sample cell reservoir to the center of the gap between the plates. From (a) to (c) the wetness increases as d gets smaller. The images show the surface Plateau borders along the top plate of the sample cell. The thick surface Plateau borders along the top plate are connected to slightly thicker ones along the bottom plate by thin films. Three surface Plateau borders meet at a surface vertex. The vertices appear bright due to light channeled through vertical Plateau borders that span the gap between both plates.

2D foam is the Plateau border radius r in comparison with the gap H.

B. Image analysis

After the foam is prepared it is immediately placed 75 cm above a Vista Point A light box and 12.5 cm below a Nikon D90 camera with a Nikkor AF Micro 105mm 1:2.8D zoom lens. The lens is set to full zoom and the entire field of view is 23.3×15.4 mm^2. The location of the camera is optimized to have the smallest absolute field of view while also keeping the foam in focus, which allows us to devote as many pixels as possible to any individual bubble. This limits the total numbers of bubbles we can reconstruct in each image, but each bubble will have very accurate measurements of its area. An image is taken every minute for a minimum of 24 h, but only images of the foam after it coarsens to a quasi-2D state are kept for analysis. Once the foam enters this state, we must identify the bubbles in each image to find their shapes and areas. The latter can ostensibly be done
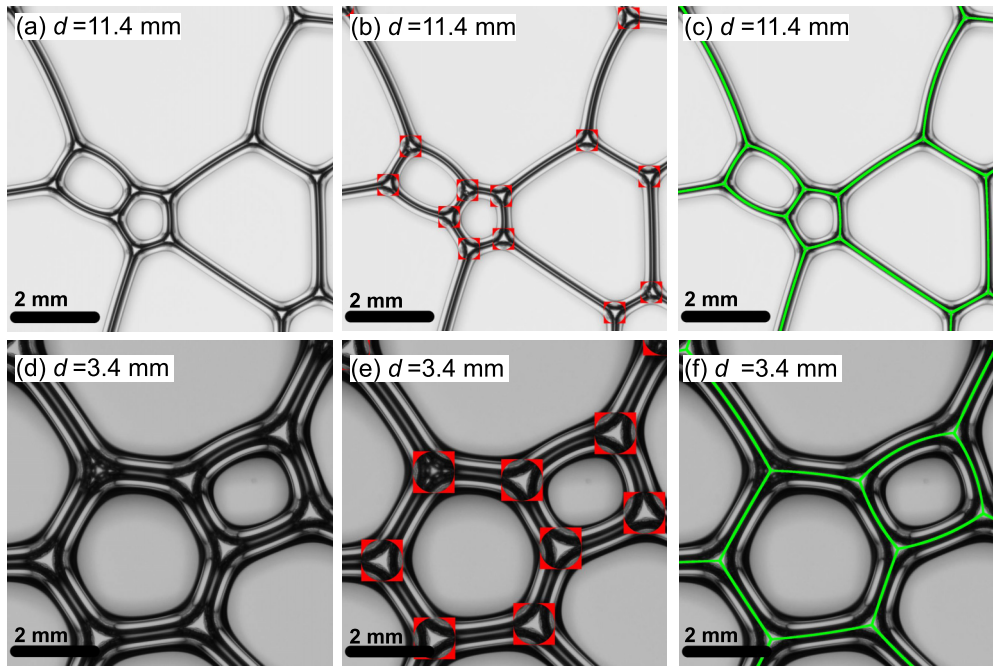
FIG. 2. Three stages of the foam reconstruction for foams of two different wetnesses as indicated by d. (a), (d) The raw data. (b), (e) Locations and orientations of the vertices determined by a Monte Carlo-like method described in the Supplemental Material [24]. (c), (f) The circular arcs that connect pairs of vertices as thick green lines. These arcs reconstruct the film network, and they match well with the middle of corresponding surface Plateau borders.

by binarizing, skeletonizing, and watershedding the pictures of the foam. However, our images have features of varying brightness that make the skeletonized images poor representations of the foam and the subsequent watershed basins invalid for measuring the area of bubbles. Instead we have developed an algorithm for reconstructing these wet foams where we find the (x, y) locations of the vertices as well as the orientation of one of the three surface Plateau borders of the vertex with respect to the x-axis. For brevity we show our vertex finding method works by displaying in Fig. 2 the found locations of the vertices; the method finds neither false positive nor false negatives locations of vertices such that every bubble we reconstruct has only n sides throughout its lifetime. The Supplemental Material thoroughly explains the algorithm for finding the vertices and why it is necessary over more usual watershedding methods; also included is a movie that demonstrates the vertex identifying process [24].

The orientations of the surface Plateau borders belonging to a vertex are used to identify the network of neighboring vertices. We know from Plateau's laws that the films in 2D and surface Plateau borders in quasi-2D foams are separated at a vertex by an angle of $120°$. Therefore knowing the orientation of one surface Plateau border informs us of the directions of the others. We know precisely where to investigate in order to find the three neighbors of a vertex. After the neighbors are determined for each vertex, we connect them to recreate the film network of the foam.

Another of Plateau's laws is that films connecting the vertices in quasi-2D foam are arcs of circles. The center and radius $(x_c, y_c, \mathcal{R})$ of the circles that connect any pair of vertices are defined by the vertex locations and a point midway between the two vertices in the middle of the surface Plateau

border. The method used to determine this third point is presented in the Supplemental Material [24]. Additionally the reconstructed film network is adjusted to better satisfy Plateau laws; explanations of this process and a movie representing the evolution of the reconstructions are also included in the Supplemental Material [24]. In Figs. 2(c) and 2(f) we show the circular arcs that reconstruct the film network.

With the film network carefully reconstructed we can finally determine the areas and shapes of the coarsening bubbles. We first identify which vertices belong to a bubble. The bubble area is then calculated in two steps using, first, the location of the vertices and then using the equations of the circular arcs that connect them. The bubble is initially treated like a polygon where the vertices are connected by straight lines. This treatment gives a polygonal area of $\alpha = \sum (x_i y_{i+1} + x_{i+1} y_i)/2$ where the sums are between all pairs of connected vertices belonging to a bubble. Because the vertices are actually attached by arcs of circles and not straight lines, we then account for the area under the circular arcs; the bubble area is in total its polygonal area plus or minus the area under each of the n circular arcs of the bubble if the arc bends away or towards the centroid of the bubble, respectively. Once the bubble area is known we use it along with the values of $\mathcal{R}$ for each of the n sides of the bubble to evaluate Eq. (3). This is done for all bubbles in an image and for all images.

Finally we measure the uncertainty in the areas and circularities. These uncertainties account for how well the foam is reconstructed, and to determine them we refit the films connecting neighboring vertices. We refit on three points: two of the points are the vertex locations slightly shifted so the distance between them increases; the third remains in the bright band in the middle of the film but is shifted to maximize
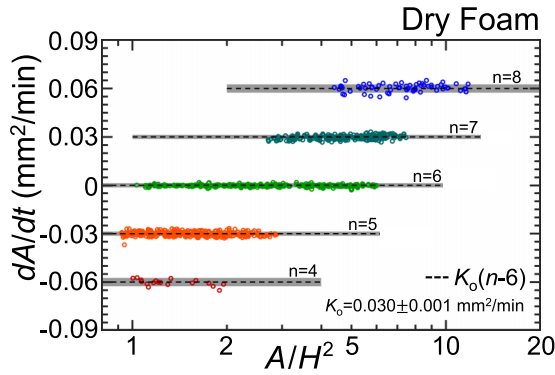
FIG. 3. Rate of change of bubble area A versus A divided by the square of the gap H between plates, for a dry foam consisting of bubbles with different numbers of sides as labeled by n. Each point represents the data for one bubble, and there are data for 1533 bubbles. The von Neumann expectation $dA/dt = K_o(n-6)$ is plotted for $K_o = 0.030 \pm 0.001$ mm²/min, as shown by horizontal dashed lines and gray swaths.

the distance from each vertex. This provides values for the center and radius $(x'_c, y'_c, \mathcal{R}')$, and these are used to find areas A' and circularities C'. The values of A' and C' are used only to determine the uncertainties which are then $\Delta A = A - A'$ and $\Delta C = C - C'$; in these equations A and C are the originally calculated values of the area and circularity of each bubble, and all data presented in upcoming figures are $A \pm \Delta A$ and $C \pm \Delta C$. Once the areas, circularities, and uncertainties for each are calculated, all bubbles are tracked using standard particle-tracking procedures.

III. COARSENING RATES

Having tracked individual bubbles, we observe how their areas change throughout their lifetime. Recall that von Neumann's law says for 2D dry foams that the coarsening rate of a bubble should depend only on its number of sides; bubbles with $n > 6$ grow, bubbles with $n < 6$ shrink, and bubbles with $n = 6$ do not have their area change. Equation (2) generalizes coarsening behavior for quasi-2D wet foams where the wetness of the foam along with the size and shape of a bubble will have an effect. Coarsening rates for bubbles in a quasi-2D geometry are shown in Fig. 3 for foams that are effectively dry and in Fig. 4 for wet foams of varying liquid content.

To test for von Neumann-like behavior we make dry foams by standing the sample cell so that the plane of the foam is vertical. Drainage results in all the liquid pooling to the bottom of the cell and bubbles far from the liquid do not have any enlarged Plateau borders. A very conservative estimate for this distance is 1 cm above the bath which is about 4 times the capillary length, and only bubbles this distance and above the liquid pool are analyzed. For dry foams it is easier to acquire information about the bubble areas than for the wet foams. The areas of dry bubbles are determined from a process where we binarize, skeletonize, and watershed images of the foam. Bubbles are the watershedding basins of the skeletonized images, and the number of pixels within each basin is converted into the bubble area.
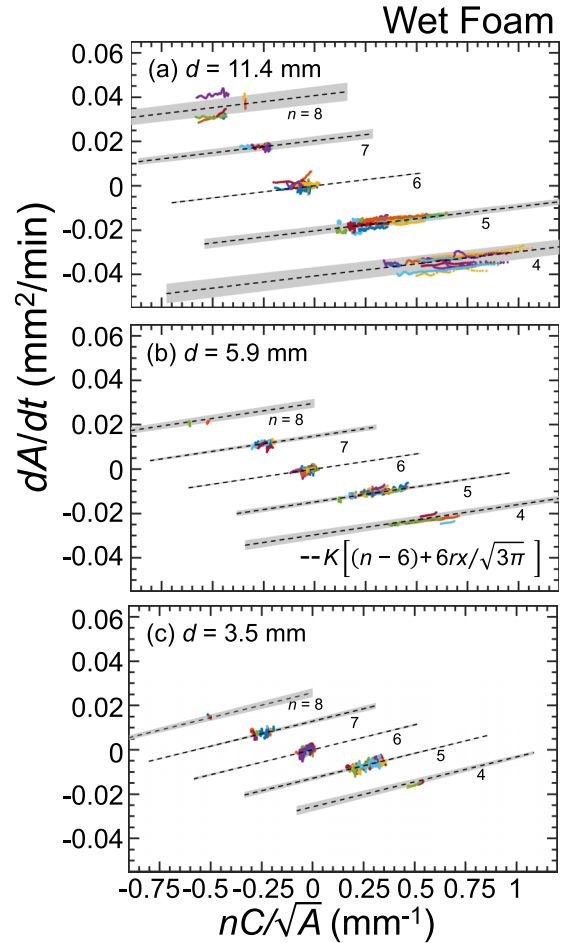

FIG. 4. Coarsening rate versus number of sides multiplied by the circularity and divided by the square root of the area of individual bubbles; data are shown for wet foams with various liquid content as labeled by d. Coarsening data for individual bubbles are shown as colored dots, and in panels (a), (b), and (c) there are data for $N =$ [63, 90, 68] bubbles, respectively; the x-axis values are calculated using the bubble-specific values of $C(t)/\sqrt{A(t)}$. The black dashed lines show the expectation for the generalized coarsening equation; they are evaluated by making simultaneous fits to the coarsening rates for all bubbles in each wetness where the reduced coarsening rate K and the average radius of curvature of the Plateau borders r are fit parameters. The gray swaths show the equation evaluated using $K \pm \Delta K$ and $r \pm \Delta r$.

Individual bubble tracks show areas that change linearly with time, and to find the coarsening rate for each bubble we fit lines to the data. The values of dA/dt are plotted versus bubble area in Fig. 3. It is evident that the coarsening rates are the same for all bubbles with the same number of sides, and the choice of x-axis shows this is true regardless of the size of the bubble. The coarsening rates for n-sided bubbles follows von Neumann's law $dA/dt = K_o(n-6)$, and rate constant K_o is found to be $K_o = 0.030 \pm 0.001$ mm²/min.

Turning to our main interest in wet foams, we find by contrast with the dry case that bubbles with the same number of sides do not all coarsen at the same rate. This is shown in Fig. 4, which plots dA/dt not versus area but rather versus the quantity $x = nC/\sqrt{A}$ that controls the deviation from von

$$\gamma/r_t = \rho g\left[\left(d+\tfrac{H}{2}\right) - r_t\right]$$

$$\gamma/r_b = \rho g\left[\left(d-\tfrac{H}{2}\right) + r_b\right]$$

$$— (r_t + r_b)/2$$

$$— K_o\left(1 - \frac{2r}{H} + \frac{\pi\sqrt{r\ell}}{H}\right)$$
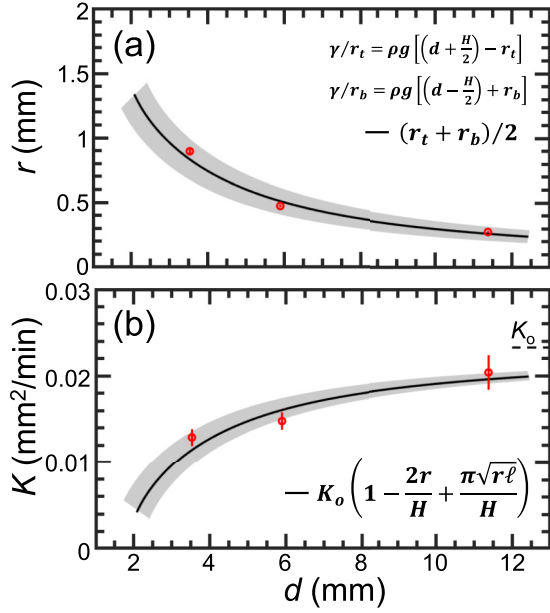
FIG. 5. The average Plateau border radius (a) and reduced coarsening rate (b) versus the distance d from top surface of liquid in the sample cell reservoir to the center of the gap between the plates. Data are shown as points, and expectations are shown as solid curves with a gray swath reflecting uncertainty in γ, ρ, d, and ℓ. In panel (b) the value of K_o used to evaluate the expectation is plotted as a dashed line. Note that as d increases, the foam becomes drier and hence r decreases, and K increases in good accord with expectation.

Neumann behavior in Eq. (2); unlike the data for the dry foams, the coarsening rates for individual bubbles in a wet foam will be affected by their size as well as their shape, and this is in accordance with our generalized coarsening equation. Thus the choice for the x-axis is appropriate and their values are determined from the raw values of $C(t)$ and $A(t)$ taken for individual bubble tracks, as well as the number n of sides found from the reconstruction of the network. The coarsening rates on the y-axis are the numerical derivatives of the area data smoothed over a Gaussian window. Indeed, we find in Fig. 4 that dA/dt is not constant for a given n but rather varies linearly in x as predicted. Also as predicted, the slope varies with wetness independent of n. Thus there is good qualitative agreement with expectation, which may now be tested more quantitatively:

According to Eq. (2), the separation and slope of the data clusters are set, respectively, by the values of $K = K_o(1 - 2r/H + \pi\sqrt{r\ell}/H)$ and the average radius of curvature r of the surface Plateau border. To find K and r, these parameters are adjusted to simultaneous fit the coarsening rates for all the bubbles in each wetness. Excellent fits are achieved, as illustrated by the dashed lines in Fig. 4. The gray swaths show the fitting equation evaluated across the acceptable range of fitting parameters, $K \pm \Delta K$ and $r \pm \Delta r$.

To complete the analysis, the fitting parameter results are plotted versus, d, the distance from top surface of liquid in the sample cell reservoir to the center of the gap between the plates which controls wetness, and compared with expectation in Fig. 5. In Fig. 5(a), results for the average Plateau border radius r decrease with increasing d for drier foams.

The expectation for r is shown as a solid curve surrounded by a gray swath that represents the uncertainties in γ, ρ, and d. There are no fitting parameters, and even so the agreement is very good. In Fig. 5(b) results for K increase with increasing d for drier foams, and the expectation is similarly shown. Now the overall rate K_o is adjusted to give a good fit to the data. This yields $K_o = 0.023 \pm 0.002$ mm^2/min, taking the film thickness from across a reasonable wide range of values, 10^{-5} mm $< \ell < 10^{-3}$ mm [25–27]. The result is somewhat smaller than the value $K_o = 0.030 \pm 0.001$ mm^2/min measured in Fig. 3 for a perfectly dry foam using the usual von Neumann equation. The source of discrepancy is not known, but could arise by a slight change in the physical chemistry of the solution. Nevertheless, the parameters r and K give excellent fits in Fig. 4 to the expected variation with wetness, further demonstrating the validity of the generalized coarsening equation.

IV. INDIVIDUAL BUBBLE COARSENING

In this final section we highlight that bubble shape drives the deviations from von Neummann's law, by returning to the raw data for bubble area and circularity versus time for a few individual bubbles in the above analyses. We begin with six-sided bubbles, some of which grow and some of which shrink as seen by careful inspection of the sign of dA/dt data in Fig. 4. This effect, and its analog for $n \neq 6$, is more obvious and dramatic in $A(t)$ versus t data for individual bubbles as follows.

A. Bubbles with $n = 6$

According to von Neumann's law, the area of six-sided bubbles in a dry foam should not change in time. By contrast, for wet foams, the expectation of Eq. (2) for six-sided bubbles reduces to $dA/dt = 6KnrC(t)/\sqrt{3\pi A(t)}$. Therefore, sign of the circularity shape parameter $C(t)$ and the magnitude of $C(t)/\sqrt{A(t)}$ determines whether a six-sided bubble grows or shrinks and at what rate. Data for the area of examples bubbles in foams of various wetness are shown in Fig. 6, where the area is seen to either decrease as in Figs. 6(a) and 6(b) or to grow as in Fig. 6(c). The corresponding circularities are plotted in Figs. 6(d)–6(f). There we see $C(t) < 0$ in Figs. 6(d) and 6(e) for bubbles that shrink and $C(t) > 0$ in Fig. 6(f) for the bubble that grows. This shows there is good qualitative agreement with Eq. (2) and the coarsening behavior. Additional data in the Supplemental Material for $A(t)$ and $C(t)$ versus time [24] show more examples of qualitative agreement between the change in area and bubble shape for many six-sided bubbles from foam with $d = 5.9$ mm.

To demonstrate the quantitative validity of Eq. (2) for dA/dt for these three six-sided bubbles, we numerically integrate it using the displayed $C(t)$ data in order to obtain $A(t)$ versus t along with the fitted values of K and r discussed above. The resulting predictions for $A(t)$ versus t are displayed as dashed curves with a surrounding gray swath that reflects statistical uncertainties in K, r, and C. Evidently, the agreement is remarkably good. Of course this is expected based on the success of the fits in the previous figures. Nevertheless it is a powerful demonstration that von Neumann's
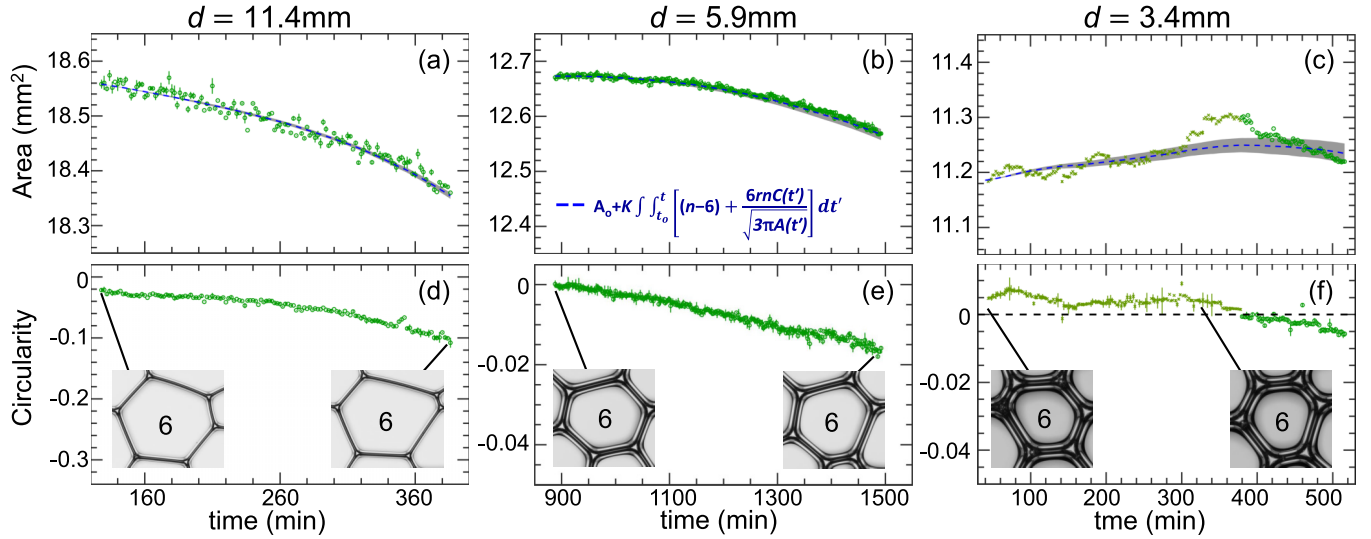
FIG. 6. The area (a)–(c) and circularity (d)–(f) versus time for individual six-sided bubbles. The bubbles come from foams of increasing wetness from left to right as labeled by decreasing d. The images in panels (d)–(f) show the bubble at the times pointed to by the black lines. The von Neumann expectation is that six-sided bubbles do not change their area in time, but panels (a) and (b) show six-sided bubbles that shrink, and panel (c) shows a bubble that initially grows and eventually shrinks. These area changes are driven by the bubble circularity, which is negative at all times in panels (a) and (b) and positive during the bubble growth in panel (c); in all parts the data are represented by dark green circles except in panels (c) and (d) when the bubble is growing or has positive circularity, then the data are plotted with a light green ×. The blue dashed lines are the numerically integrated solutions to the generalized coarsening equation using the bubble circularity data as well as values of K and r corresponding to the bubble wetness. The gray swaths are generated similarly, incorporating statistical uncertainty in C as well as uncertainty in the values of K and r. In panel (f) the black dashed line shows where $C = 0$.

law is indeed violated for wet foams according to prediction in terms of the bubble shape. Note that the agreement is accurate at the level of ≈ 0.01 mm, and that the comparison was made possible by the high precision of our data.

These results raise a new question: What controls the value and time evolution of a bubble's circularity shape parameter and hence whether A grows or shrinks? To begin exploring this issue, we examine the photographs of the example bubbles shown in Fig. 6 at early and late times. In these it is not possible to visually discern the area changes. But, in Fig. 6(d), it is nevertheless apparent that the shortest side becomes much shorter and more highly negatively curved. Since the Eq. (3) definition of C features an unweighted sum of curvature for each side, the very short, very curved film contributes very strongly to C, and hence is responsible for it being both negative and a decreasing function of time. More generally, six-sided bubbles often have a small few-sided bubble as neighbor that shares a short film that shrinks and becomes more curved with time. Thus we find $C(t)$ tends to be negative and decreasing for many six-sided bubbles. Six-sided bubbles with $C > 0$, that grow with time as in Fig. 6(c), exist but are more rare. We leave it to future studies to further consider the distribution and evolution of shape parameters in terms of nearest-neighbor size and shape correlations.

B. Bubbles with $n \neq 6$

While the way bubble shape drives violation of the von Neumann law is most evident for six-sided bubbles, it can also be seen for bubbles with other side numbers n. According to Eq. (2) the coarsening rates for bubbles with the same n are different from one another depending on the individual bubble

shape; how the circularity of a bubble affects its coarsening is demonstrated qualitatively in the Supplemental Material with plots showing $A(t)$ and $C(t)$ versus time for many n-sided bubbles from foam with $d = 5.9$ mm [24].

Quantitatively this is demonstrated for one five-sided and one seven-sided bubble in Fig. 7 and for other bubbles in the Supplemental Material [24]. Just as in Fig. 6, the top and bottom rows, respectively, show area and circularity data versus time, along with photographs of the bubbles at early and late times. For $n = 5$ and for $n = 7$ the bubbles respectively shrink and grow, nearly linearly with time as expected from the von Neumann law. Indeed the area change is evident in the photographs. However, in both cases the area change is slightly slower than linear. And, in fact, this deviation is perfectly captured by numerical integration of the coarsening equation using the $C(t)$ data, exactly as done for the six-sided examples. Now the sign of the deviation is more clear: Five-sided bubbles always have positive circularity, while $(n - 6)$ is negative; therefore they shrink more slowly than in the von Neumann law. Similarly, seven-sided bubbles always have negative circularity, while $(n - 6)$ is positive; therefore they grow more slowly than in the von Neumann law. For the example $n = 5$ bubble, the circularity is roughly constant as it shrank. By contrast, the circularity of $n = 7$ example bubble decreased as two of its shorter sides became even shorter and more curved, similar to what was seen for typical $n = 6$ bubbles.

V. CONCLUSION

In this work we show that the generalized coarsening equation describes the coarsening behavior of bubbles in a wet
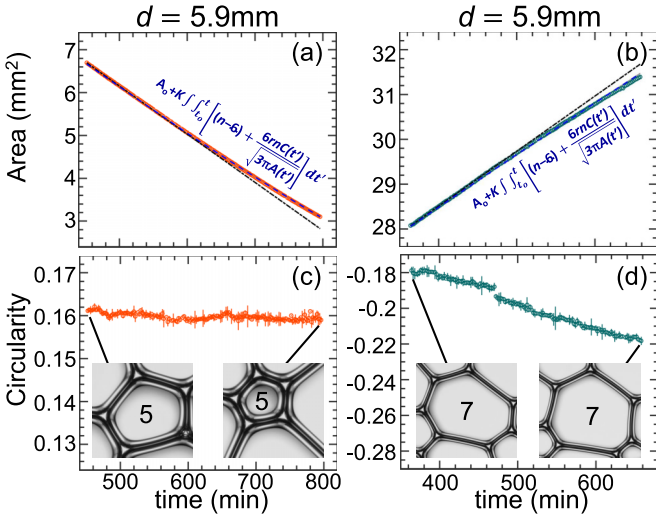
FIG. 7. The area (a)–(b) and circularity (c)–(d) versus time for individual bubbles with n number of sides as labeled in the bubble images; both bubbles come from a foam with the same wetness indicated by d. The images in panels (c) and (d) show the bubble at the times pointed to by the black lines. In panels (a) and (b) the black dash-dotted lines are tangent to the data at early times and demonstrate the area changes for these bubbles is nonlinear. This behavior is due to the bubble circularity where five- or seven-sided bubbles shrink or grow more slowly because $C(t) > 0$ or $C(t) < 0$, respectively. The blue dashed lines are the numerically integrated solutions to the generalized coarsening equation using the bubble circularity data as well as values of K and r corresponding to the bubble wetness. The gray swaths are generated similarly, incorporating statistical uncertainty in C as well as uncertainty in the values of K and r.

foam and predicts changes to the area of individual bubbles. This is some of the most precise data taken of coarsening bubbles, and very small changes in bubble area are accurately measured. This becomes increasingly important when considering how small in magnitude the area changes are for six-sided bubbles. To show the average behavior follows Eq. (2), we make a simultaneous fit to the data of different n-sided bubbles where the fit parameters are the reduced coarsening rate K and the radius of curvature of the Plateau borders r. The r values from the fit agree with the calcu-

lated values of r values determined from Eqs. (5) and (4). A mystery remains why the K values from the fit are somewhat different from the expected values; still the K values from the fit decrease monotonically with increasing wetness and are predicted if $K_o = 0.023$ mm^2/min. We show that dA/dt is not constant for any set of n-sided bubbles but instead depends on the individual bubble shape and size.

Using these parameters we show how Eq. (2) also predicts the coarsening behavior of individual bubbles. In particular the coarsening of six-sided bubbles, which is not predicted by von Neumann's law, is determined exclusively by the bubble shape. We show this by solving Eq. (2) through numerical integration of the circularity data for several six-sided bubbles from foams of different wetness. The data show the six-sided bubbles coarsen with rate changes depending on their shape, and this is matched by solutions to the generalized coarsening equation. The shape changes that drive the coarsening rate changes are easily visualized, especially for shrinking six-sided bubbles, from changes in the film network that cause changes in circularity. Coarsening six-sided bubbles are the most obvious violations of von Neumann's law, but other n-sided also have their coarsening rates reduced due to shape effects. In some cases this leads to obvious nonlinear behavior.

Further verification of our generalized coarsening equation is possible by working with a hexagonal packing of bubbles, which can be accomplished with a specialized cell with hexagonal boundary conditions. If all bubbles are six-sided, then any observed coarsening both is in violation of von Neumann's law and would necessarily be due to the bubble circularity. Additionally future work could continue to increase the liquid volume fraction of the foam to study systems that are "very wet" where there is a breakdown of Plateau's laws and bubbles are separated only by liquid faces. The coarsening behavior of these foams is predicted in Ref. [20], but this equation is not yet tested experimentally. Coarsening also necessarily relaxes the system and induces rearrangements [28]. While this study focuses on the dynamics of coarsening, we can also study bubble rearrangements in both dry and wet foams brought on by coarsening.

[1] D. Weaire and S. Hutzler, *The Physics of Foams* (Oxford University Press, New York, 2001).

[2] I. Cantat, S. Cohen-Addad, F. Elias, F. Graner, R. Höhler, O. Pitois, F. Rouyer, and A. Saint-Jalmes, *Foams: Structure and Dynamics* (Oxford University Press, Oxford, 2013).

[3] J. A. Glazier and D. Weaire, The kinetics of cellular patterns, J. Phys.: Condens. Matter **4**, 1867 (1992).

[4] J. Stavans, The evolution of cellular structures, Rep. Prog. Phys. **56**, 733 (1993).

[5] J. von Neumann, *Metal Interfaces* (American Society of Metals, Cleveland, 1952), pp. 108–110.

[6] J. Stavans and J. A. Glazier, Soap Froth Revisited: Dynamic Scaling in the Two-Dimensional Froth, Phys. Rev. Lett. **62**, 1318 (1989).

[7] J. Stavans, Temporal evolution of two-dimensional drained soap froths, Phys. Rev. A **42**, 5049 (1990).

[8] J. Stavans, Evolution of two-dimensional cellular structures: The soap froth, Physica A **194**, 307 (1993).

[9] M. de Icaza, A. Jiménez-Ceniceros, and V. M. Castaño, Statistical distribution functions in 2D foams, J. Appl. Phys. **76**, 7317 (1994).

[10] J. A. Glazier, M. P. Anderson, and G. S. Grest, Coarsening in the two-dimensional soap froth and the large-Q Potts model: A detailed comparison, Philos. Mag. B **62**, 615 (1990).

[11] T. Herdtle and H. Aref, Numerical experiments on two-dimensional foam, J. Fluid Mech. **241**, 233 (1992).

[12] D. Segel, D. Mukamel, O. Krichevsky, and J. Stavans, Selection mechanism and area distribution in two-dimensional cellular structures, Phys. Rev. E **47**, 812 (1993).

[13] A. D. Rutenberg and M. B. McCurdy, Scaling state of dry two-dimensional froths: Universal angle-deviations and structure, Phys. Rev. E **73**, 011403 (2006).

[14] L. Neubert and M. Schreckenberg, Numerical simulation of two-dimensional soap froth, Physica A **240**, 491 (1997).

[15] F. Bolton and D. Weaire, The effects of plateau borders in the two-dimensional soap froth I. Decoration lemma and diffusion theorem, Philos. Mag. B **63**, 795 (1991).

[16] A. E. Roth, C. D. Jones, and D. J. Durian, Bubble statistics and coarsening dynamics for quasi-two-dimensional foams with increasing liquid content, Phys. Rev. E **87**, 042304 (2013).

[17] J. A. Glazier and J. Stavans, Nonideal effects in the two-dimensional soap froth, Phys. Rev. A **40**, 7398 (1989).

[18] J. Marchalot, J. Lambert, I. Cantat, P. Tabeling, and M.-C. Jullien, 2D foam coarsening in a microfluidic system, Europhys. Lett. **83**, 64006 (2008).

[19] J. A Marqusee, Dynamics of late stage phase separations in two dimensions, J. Chem. Phys. **81**, 976 (1984).

[20] C. D. Schimming and D. J. Durian, Border-crossing model for the diffusive coarsening of two-dimensional and quasi-two-dimensional wet foams, Phys. Rev. E **96**, 032805 (2017).

[21] J. A. Glazier, S. P. Gross, and J. Stavans, Dynamics of two-dimensional soap froths, Phys. Rev. A **36**, 306 (1987).

[22] Y. Seol and Y. Kim, Numerical study on statistical behaviors of two-dimensional dry foam, Commun. Comput. Phys. **25**, 289 (2018).

[23] I. Fortuna, G. L. Thomas, R. M. C. de Almeida, and F. Graner, Growth Laws and Self-Similar Growth Regimes of Coarsening Two-Dimensional Foams: Transition from Dry to Wet Limits, Phys. Rev. Lett. **108**, 248301 (2012).

[24] See Supplemental Material at http://link.aps.org/supplemental/10.1103/PhysRevE.103.012610 for additional details on the experimental materials and reconstruction methods as well as a video and analyses of more bubbles.

[25] V. Bergeron and C. J. Radke, Equilibrium measurements of oscillatory disjoining pressures in aqueous foam films, Langmuir **8**, 3020 (1992).

[26] P. Kralchevski, A. Nikolov, D. T. Wasan, and I. Ivanov, Formation and expansion of dark spots in stratifying foam films, Langmuir **6**, 1180 (1990).

[27] Y. Zhang and V. Sharma, Nanoridge formation and dynamics of stratification in micellar freestanding films, Langmuir **34**, 1208 (2018).

[28] A. D. Gopal and D. J. Durian, Relaxing in Foam, Phys. Rev. Lett. **91**, 188303 (2003).